Inverted Vibrational and Rotational Excitation of CN(B 2 Σ +) Produced through Superexcited Ion-Pair States of MCN (M = Na, K, Rb)

Hisato Yasumatsu, Gwang-Hi Jeung

Inverted Vibrational and Rotational Excitation of CN($B^2\Sigma^+$) Produced through Superexcited Ion-Pair States of MCN (M = Na, K, Rb)

Hisato Yasumatsu* and Gwang-Hi Jeung

ABSTRACT: This paper reports an energy-partition mechanism in dissociative excitation of alkali cyanide molecules, MCN (M = Rb, K, Na), to produce CN($B^2\Sigma^+$) and M(ns^2S) (n = 5, 4, and 3 for Rb, K, and Na, respectively) in collision with Kr metastable atoms, $Kr^m(^3P_{2,0})$. Both the vibrational and rotational distributions of CN($B^2\Sigma^+$) produced in the reactions of RbCN and KCN were inverted as being peaked at v' = 1 and N' = 35, respectively, where v' and N' are the vibrational and the rotational quantum numbers of CN($B^2\Sigma^+$), respectively. According to a state crossing model, it was derived that CN($B^2\Sigma^+$) is produced by predissociation through a superexcited ion-pair state, $CN^-(3^1\Sigma^+)\cdot M^+(^1S)$, followed by an adiabatic transition to a repulsive state correlating to the dissociation limit of CN($B^2\Sigma^+$) + M(ns^2S). The inverted distributions are driven by structural changes during the excitation and the adiabatic transition. The maximum vibrational population at v' = 1 originates from a large Franck−Condon overlap between the vibrational wavefunctions of $CN^-(3^1\Sigma^+)$ and CN($B^2\Sigma^+$) at v' = 1. The rotational excitation of the CN($B^2\Sigma^+$) product is explained with changing from a T-shape geometry of MCN in the ground state to a linear one in the superexcited ion-pair state.

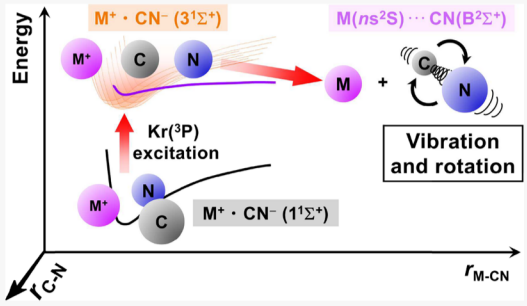

I. INTRODUCTION

In chemical reactions via electronically excited states, reaction products and partition of the excess energy into degrees of freedom of the products are specific and characteristic to the initial, intermediate, and/or final states. The change in the geometric structure during the reaction is one of the key factors to determine the final products and energy partition. Particularly, reactions through superexcited states, which possess higher internal energy than the electron-detachment energy, result in characteristic products and energy partition, since both of their high excess energy and high density of states lead to numbers of reaction paths.[1,2] Most of previous studies on reactions through superexcited states were, however, reported for covalent molecules, and knowledge for ionic-bonding molecules is limited.

Alkali cyanides or isocyanides, MCN or MNC (M = alkali metal), are representative triatomic ionic-bonding molecules.[3−5] By an analogy of the alkali halide molecules, MCN has a large number of ion-pair and covalent states correlating to the asymptotic dissociation limits of $M^+ + CN^-$ and M + CN, respectively, where M is in the Rydberg series converging to M^+, CN^- is in the electronic states of $X(^1\Sigma^+)$, $2(^1\Sigma^+)$, $3(^1\Sigma^+)$, etc., and CN is in $X(^2\Sigma^+)$, $A(^2\Pi)$, $B(^2\Sigma^+)$, etc.[6] Indeed, the absorption bands and peaks observed in the photoabsorption spectra of MCN in a vacuum ultraviolet region have been assigned to the excited ion-pair and covalent repulsive states, respectively.[7] Considering the ionization energies of MCN (~10 eV)[3] and attractive Coulomb energy between M^+ and CN^-, the excited states correlating to $M^+ + CN^-(2^1\Sigma^+)$, $M^+ + CN^-(3^1\Sigma^+)$, and higher states are recognized as superexcited states of MCN;[7] it is noted that $CN^-(2^1\Sigma^+)$ and $CN^-(3^1\Sigma^+)$ are also in superexcited states as they are located above the electron affinity of CN; the electronic energies of $CN^-(2^1\Sigma^+)$ and $CN^-(3^1\Sigma^+)$ were calculated as 6.386 and 7.524 eV, respectively,[6] both of which are larger than the electron affinity of CN, 3.86 eV. Owing to high density of states of M in the Rydberg states as well as the electronically excited states of CN and CN^-, the potential energy surfaces of the superexcited states of MCN experience many avoided crossings, as our ab initio calculation on LiNC displayed many diabatic couplings among these states.[6] These diabatic couplings are of significant importance in determining the reaction dynamics and the energy partition through the superexcited states.

In our previous studies on the dissociative excitation of MCN by collisional energy transfer from argon metastable atoms, $Ar^m(^3P_{2,0})$ (excitation energies are 11.55 and 11.72 eV), we have discovered two reaction channels for the production

of $CN(B^2\Sigma^+)$: direct dissociation on a repulsive state correlating to $CN(B^2\Sigma^+) + M(ns^2S)$ (n = 5, 4, and 3 for Rb, K, and Na, respectively) and predissociation through a superexcited ion-pair state consisting of M^+ and a superexcited cyanide, $[CN^-]^{**}$, followed by adiabatic transition to the repulsive state.[8,9] The predissociation results in a selective energy partition such that 90% of the energy available for the reaction products is transferred into the vibrational degree of freedom of the $CN(B^2\Sigma^+)$ product ($v' = 11-19$), where v' is a vibrational quantum number of $CN(B^2\Sigma^+)$. This is in remarkable contrast to that in the direct dissociation in which ~90% of the available energy is transformed into the translational degree of freedom of the products owing to its high density of states. The characteristic vibrational distribution originates from a large Franck–Condon overlap between $[CN^-]^{**}$ and $CN(B^2\Sigma^+)$ in the $v' = 11-19$ range due to a much larger C–N internuclear distance (0.14 nm) of $[CN^-]^{**}$ involved in this predissociation than that of $CN(B^2\Sigma^+)$ (0.115 nm).[9]

The energy partition among products of dissociative excitation changes characteristically with superexcited states involved. A study on the dissociative excitation at a different excitation-energy, hence through different superexcited states, clarifies the predissociation mechanism further. In this connection, we studied dissociative excitation of MCN through superexcited states located at ~10 eV[7] initiated by collisional energy transfer from $Kr^m(^3P_{2,0})$ having the excitation energies of 9.9 and 10.6 eV for the total angular momenta of 2 and 0, respectively,

$$MCN + Kr^m(^3P_{2,0}) \rightarrow CN(B^2\Sigma^+) + M(ns^2S) + Kr(^1S), \quad (1)$$

where the M product is in the ground state in consideration of energetics. The dissociation mechanism was derived in a framework of the predissociation through a superexcited ion-pair state of MCN on the basis of the vibrational and rotational distributions of the $CN(B^2\Sigma^+)$ product determined by analyzing $CN(B^2\Sigma^+-X^2\Sigma^+)$ emission spectra measured.

II. EXPERIMENTAL SECTION

This paper presents a brief description relating to the present experiment, and the details have been described in our previous reports.[8,9] A flowing afterglow method was used to excite MCN molecules in collision with $Kr^m(^3P_{2,0})$ produced by microwave discharge (2.45 GHz, 120 W) of pure Kr gas (99.95% pure) or a gas mixture of 1% Kr diluted in Ar (99.9995% pure). An effusive beam of MCN evaporated from a tantalum crucible heated at 800–850 K at which the vapor pressure of MCN is in an order of 10^{-1} Pa.[8–10] The $CN(B^2\Sigma^+-X^2\Sigma^+)$ emission from the $CN(B^2\Sigma^+)$ fragment produced in reaction 1 was dispersed in a monochromater (SPEX 1704) and detected with a photomultiplier (Hamamatsu R585) in a photon-counting method; the resolution was 0.03 nm (FWHM) at 380 nm. The pressure of the reaction region was maintained at 6×10^{-1} Pa at which collisional relaxation of the vibration and rotation states of the $CN(B^2\Sigma^+)$ product can be disregarded within the emission lifetime of $CN(B^2\Sigma^+)$.[11]

A concentration ratio of the two spin-orbit states of Kr^m, $[Kr(^3P_2)]/[Kr(^3P_0)]$, was determined to be 7 and 40 in the discharged pure Kr gas and the Kr/Ar mixture, respectively, by observing $CO(d^3\Delta-a^3\Pi)$, $CO(a'^3\Sigma^+-a^3\Pi)$, $CO(b^3\Sigma^+-a^3\Pi)$ and $CO(e^3\Sigma^--a^3\Pi)$ emissions where collision between $Kr(^3P_2)$ and CO produces mainly $CO(d^3\Delta)$ and $CO(a'^3\Sigma^+)$, while $Kr(^3P_0)$ produces mainly $CO(b^3\Sigma^+)$ and $CO(e^3\Sigma^-)$.[12] In the present experimental condition, only Kr^m contributes to the production of $CN(B^2\Sigma^+)$ in the dissociative excitation of MCN because (1) ionic species in the Kr and Kr/Ar discharge flows were successfully removed by static electric potentials applied to a set of grids located between the exit aperture of the discharge tube and the reaction region,[8,9] (2) electrons produced by Penning ionization of MCN in collision with Kr^m are negligible according to the experiment with an electron scavenger,[8] and (3) a concentration of Ar^m in the discharged Kr/Ar flow is negligibly small because the $CN(B^2\Sigma^+-X^2\Sigma^+)$ emission from $CN(B^2\Sigma^+, v' = 11-19)$ produced by the reactions of RbCN and KCN with Ar^m[8,9] was not observed.

Commercially available powder samples of NaCN and KCN (Wako Chemical Co., 97.5 and 96% pure, respectively) were employed,[8,9] while a RbCN sample was synthesized by a neutralization reaction between rubidium hydroxide and hydrogen cyanide;[9,13] an elemental analysis shows that the RbCN sample thus synthesized was 90% pure with small amounts of organic solvents used in the synthesis.[9] These impurities and water adsorbed in the samples were removed by heating them at ~400 K for more than 10 h under an ambient pressure of 1×10^{-2} Pa prior to the reaction experiment.

III. RESULTS

Figure 1 shows the $\Delta v = 0$ sequence of the $CN(B^2\Sigma^+-X^2\Sigma^+)$ emission spectra observed in the reactions of MCN with Kr^m

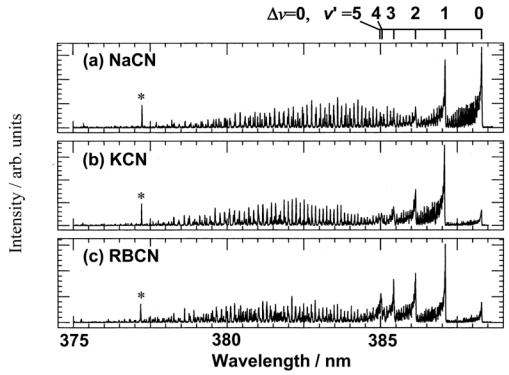

Figure 1. Emission spectra of $CN(B^2\Sigma^+-X^2\Sigma^+)$ $\Delta v = 0$ sequence observed in dissociative excitation of (a) NaCN, (b) KCN, and (c) RbCN in collision with $Kr(^3P_{2,0})$ where v' is a vibrational quantum number of $CN(B^2\Sigma^+)$. The line marked with * denotes a resonant emission line of Kr.

with the pure Kr discharge. The uncertainty of 5% in the emission intensity originates from the statistical errors. The $CN(B^2\Sigma^+-X^2\Sigma^+)$ emission spectra did not change with the concentration ratio of the two spin-orbit states of Kr^m. Therefore, on the basis of the presumable assumption that $Kr(^3P_2)$ dominantly contributes to the $CN(B^2\Sigma^+)$ production in the present reactions, the available energies, E_{av}, of the reaction

$$MCN + Kr^m(^3P_2) \rightarrow CN(B^2\Sigma^+) + M(ns^2S) + Kr(^1S) \quad (2)$$

are calculated to be 2.0 ± 0.2, 2.0 ± 0.2 and 2.1 ± 0.3 eV for RbCN, KCN, and NaCN, respectively, using the bond-dissociation energy of MCN.[14]

The vibrational and rotational distributions of the $CN(B^2\Sigma^+)$ product were obtained by simulation analysis of the

emission spectra described in ref 8. Figure 2 shows the vibrational population, $P_v(v')$, of the $CN(B^2\Sigma^+,v')$ product

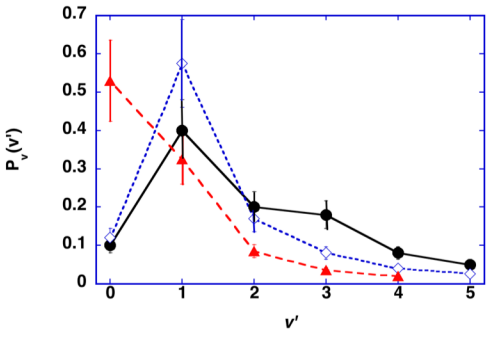

Figure 2. Vibrational populations, $P_v(v')$, of $CN(B^2\Sigma^+)$ produced in dissociative excitation of RbCN (circle solid), KCN (tilted square open) and NaCN (triangle up solid) in collision with $Kr(^3P_{2,0})$ where v' is a vibrational quantum number of $CN(B^2\Sigma^+)$. The bars indicate errors.

where the sum of $P_v(v')$ is normalized to be unity. Uncertainties of ±20% in the vibrational population shown as the bars in Figure 2 originate mainly from ambiguity in the simulation analysis. The vibrational distributions in the reactions of RbCN and KCN are inverted; the vibrational population at $v' = 1$ is larger than that at $v' = 0$. The $CN(B^2\Sigma^+)$ product in the dissociative excitation of NaCN is also considered to be vibrationally excited, as the vibrational population at $v' = 1$ is more than half of that at $v' = 0$.

The rotational distributions of the $CN(B^2\Sigma^+)$ product were identical in any vibrational states regardless of M within the uncertainties of the simulation analysis. Figure 3 shows the

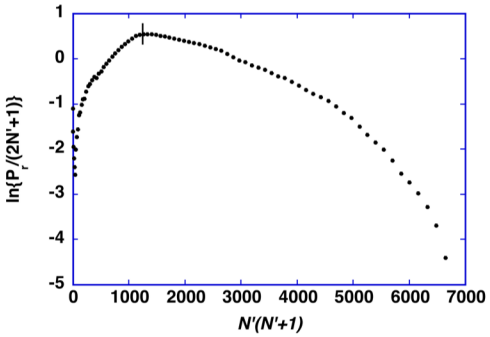

Figure 3. Boltzmann plot of rotational distribution of the $CN(B^2\Sigma^+)$ produced in dissociative excitation of MCN (M = Rb, K, and Na) in collision with $Kr(^3P_{2,0})$; natural logarithm of the rotational population, $P_r(N')$, divided by the rotational multiplicity, $2N' + 1$, as a function of $N'(N' + 1$ where N' is the rotational quantum number of $CN(B^2\Sigma^+)$. The bar indicates an error.

rotational distribution of the $CN(B^2\Sigma^+)$ product in a form of the Boltzmann plot; the natural logarithm of the rotational population, $P_r(N')$, divided by the rotational multiplicity, $2N' + 1$, is plotted as a function of $N'(N' + 1)$ where N' is the rotational quantum number of $CN(B^2\Sigma^+)$. The rotational distribution is considered to be also inverted because the Boltzmann plot of the $CN(B^2\Sigma^+)$ product deviates from a statistical linear form as well as the maximum rotational population is located at $N' \sim 35$.

IV. DISCUSSION

The inverted features observed in the vibrational and rotational distributions shown in Figures 2 and 3 originate from characteristic shapes of the potential energy surfaces involved in the dissociative excitation. The mechanisms of the inverted vibrational and rotational excitation are discussed separately in the following subsections.

IV-1. Vibrational Excitation of $CN(B^2\Sigma^+)$ Product. The extreme vibrational excitation observed cannot be explained by repulsive interactions between the fragments in direct dissociation because even the direct dissociation of MCN in collision with Ar^m, which has higher available energy than the present reaction by ~1.6 eV, results in a much less vibrational excitation of the $CN(B^2\Sigma^+)$ product than the present one.[8,9] A molecular dynamic simulation[8] also supports this consideration.

The preferential vibrational excitation has been observed in the $CN(B^2\Sigma^+)$ production by the predissociation of KCN and RbCN in collision with Ar^m.[8,9] This similarity indicates that predissociation rules also the dissociative excitation of MCN leading to the preferable vibrational excitation of the $CN(B^2\Sigma^+)$ product in collision with Kr^m, as well: MCN is excited to a predissociative superexcited ion-pair state, $[(CN^-)]^{**}\cdot M^+$, by energy transfer from Kr^m, followed by adiabatic transition to a repulsive state diabatically correlating to the dissociation limit of $CN(B^2\Sigma^+) + M(n^2S)$ in which MCN is dissociated into $CN(B^2\Sigma^+)$ and $M(ns^2S)$.

As discussed in our previous study on the dissociative excitation of MCN with Ar^m,[9] it is reasonable to consider that the vibrational distribution of the $CN(B^2\Sigma^+)$ produced in the predissociation is determined by the preferential Franck–Condon overlaps among the initial CN^-, the intermediate superexcited cyanides, $[(CN^-)]^{**}$, and the $CN(B^2\Sigma^+)$ product. According to the state-crossing model used in the previous study, the vibrational population, $P_v(v')$, of the $CN(B^2\Sigma^+)$ product is expressed as a product of the Franck–Condon factor of the CN stretching vibration and the adiabatic-transition probability between the superexcited ion-pair state and the final repulsive state as

$$P_v(v') \propto \sum_{v^g,v^e} \{|\langle v^g|v^e\rangle|^2 Q(v^e \rightarrow v')\} \tag{3}$$

where v^g and v^e are quantum numbers of the CN stretching vibration of MCN in its ground and superexcited ion-pair states, respectively, and $|v\rangle$ is a wave function of the CN-stretching vibration associated with the v'th vibrational level. The adiabatic-transition probability, $Q(v^e \rightarrow v')$, is described as[15,16]

$$Q(v \rightarrow v') = 1 - \exp\left\{-\frac{\sqrt{2}\,\pi|\langle v^e|v'\rangle|^2\alpha^2}{\sqrt{f_1 - f_2}\sqrt{\varepsilon(f_1 - f_2) + \sqrt{4\alpha^2 f^2 + \varepsilon^2(f_1 - f_2)^2}}}\right\} \tag{4}$$

where α is an interaction matrix element between the superexcited ion-pair state and the final repulsive state, ε is a relative translational energy between $[CN^-(v^e)]^{**}$ and M^+ at the crossing seam between the superexcited ion-pair state, and the final repulsive states, f_1 and f_2, are the gradients of the potential energy curves of the superexcited ion-pair state and final repulsive state, respectively, along the dissociation

coordinate, and $f = |f_1\ f_2|^{1/2}$. The potential energies of the superexcited ion-pair state and the final repulsive state were approximated by a Coulomb attractive potential and a constant potential, respectively.[9] Only such superexcited and repulsive states that cross each other at an M−CN distance longer than that of MCN in the ground state were considered. The vibrational wavefunctions, $|v^e\rangle$ and $|v'\rangle$, of the superexcited ion-pair state and the final repulsive state, respectively, were approximated by those of a bare $[CN^-]^{**}$ and $CN(B^2\Sigma^+)$, respectively, where the former was calculated by an ab initio method,[6] and the latter by the RKR method. The interaction matrix element, α, is calculated by using the Olson's method.[17] The electronic energy of $[CN^-]^{**}$, E^{**}, was used as an adjustable parameter so as to fit the experimental vibrational distribution of the $CN(B^2\Sigma^+)$ product.[9] It is sufficient to take $v^g = 0$ into consideration because the CN stretching vibration of the initial MCN is populated almost only in its ground state at the temperature of the oven (800−850 K) according to the comparison between the energy of the CN stretching vibration (~0.25 eV) and the thermal energy of the oven.

Figure 4 shows the best-fit vibrational population, $P_v^{calc}(v')$, calculated with the potential energy curve of $CN^-(3^1\Sigma^+)$ and

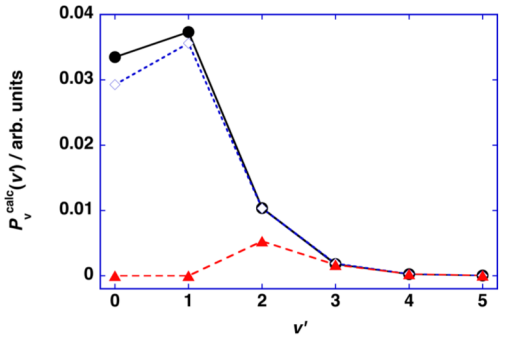

Figure 4. Calculated vibrational populations, $Pv^{calc}(v')$, of $CN(B^2\Sigma^+,v')$ produced in dissociative excitation of RbCN (circle solid), KCN (tilted square open), and NaCN (triangle up solid) in collision with $Kr(^3P_{2,0})$, by means of a state crossing model (see text) where v' is the vibrational quantum number of $CN(B^2\Sigma^+)$.

E^{**} = 7 eV. The trend of the vibrational distribution of the $CN(B^2\Sigma^+)$ product is reproduced well by the calculation for the reactions of RbCN and KCN (see Figure 2). Considering the good reproduction of the vibrational distributions with the parameter value of E^{**} = 7 eV, the predissociative superexcited ion-pair state involved is likely to be $CN^-(3^1\Sigma^+)\cdot M^+$ where the electronic energy of $CN^-(3^1\Sigma^+)$ was calculated as 7.524 eV.[6] The spin conservation during the reaction could not be strict because the spin-orbit interaction of Kr^m is relatively large so that the spin alone is not a good quantum number in the present reactions.

The inverted vibrational distribution was found to originate from a large Franck−Condon overlap, $|\langle v^e|v'\rangle|^2$, at v' = 1, owing to the larger internuclear distance between C and N of $CN^-(3^1\Sigma^+)$ (0.133 nm)[6] than that of $CN(B^2\Sigma^+)$ (0.115 nm).[18] The $CN^-(3^1\Sigma^+)$ is a superexcited state having an electron in its antibonding molecular orbital, and this is transferred to M^+ to become $M(ns^2S)$ at the adiabatic transition from the predissociative superexcited ion-pair state, $CN^-(3^1\Sigma^+)\cdot M^+$, to the repulsive state diabatically correlating to $CN(B^2\Sigma^+)$ + $M(n^2S)$. Although $CN^-(2^1\Sigma^+)$ has similar excitation energy (6.386 eV),[6] the superexcited state involving $CN^-(2^1\Sigma^+)$ can be excluded from the intermediate state of the present predissociation because the internuclear distance of $CN^-(2^1\Sigma^+)$, 0.117 nm[6] is almost the same as that of $CN(B^2\Sigma^+)$ so that the vibrational excitation would not occur.

The vibrational distribution in the reaction of NaCN was not reproduced well by this model (see Figures 2 and 4). In the model, NaCN does not result in the production of $CN(B^2\Sigma^+, v' = 0 \text{ and } 1)$, because only the potential energy curves of the superexcited ion-pair state, $CN^-(3^1\Sigma^+, v_e \leq 3)\cdot Na^+$, can cross with the final repulsive state correlating to Na + $CN(B^2\Sigma^+, v' = 0 \text{ and } 1)$ owing to the large ionization energy of Na. However, the Franck−Condon factors between $CN^-(3^1\Sigma^+, v_e \leq 3)$ and $CN(B^2\Sigma^+, v' = 0 \text{ and } 1)$ of NaCN are almost zero because of the large difference in their equilibrium CN internuclear distance. On the other hand, the superexcited ion-pair states of KCN and RbCN can cross with the final repulsive state in the range of $v_e \leq 6-7$, which has large Franck−Condon factors with $CN(B^2\Sigma^+, v' = 0 \text{ and } 1)$; the crossing point shifts to the longer M−CN distance with a decrease in the ionization energy of M; because the lower the ionization energy of M, the lower would be the energy of the superexcited ion-pair states with respect to the repulsive final states. One of the origins of the largest discrepancy for NaCN is the omission of the M-dependent Franck−Condon overlap, $|\langle v^e|v'\rangle|$,[2] in the calculation. Owing to interaction with M^+, the vibrational wavefunction, $|v^e\rangle$, of the superexcited ion-pair state is deformed from that of the bare CN^- $(3^1\Sigma^+)$ and the potential energy curve of $CN^-(3^1\Sigma^+)\cdot M^+$ along the dissociation coordinate deviates from the Coulomb one. These extents should become the largest in NaCN because the distance between $CN^-(3^1\Sigma^+)$ and Na^+ is smaller than that of RbCN and KCN owing to the smaller ionic radius of M^+.[7] The smaller difference in the ionization energy between Rb and K results in similar vibrational distributions of the $CN(B^2\Sigma^+)$ product in the reactions of RbCN and KCN.

IV-2. Rotational Excitation of $CN(B^2\Sigma^+)$ Product. The inverted rotational distribution has been observed similarly in the photodissociation of ClCN and BrCN.[19] The driving force to rotate the CN moiety in this photodissociation has been explained as large difference in the geometric structure between the ground and excited states of the parent molecules. On this analogy, the inverted rotational distribution observed in the present reaction of MCN and Kr^m is also considered originating from the geometric change from the ground state to the superexcited ion-pair state. As the equilibrium structure of MCN in the ground state is T-shape,[20−23] the superexcited ion-pair state is likely to be linear. The identical rotational distribution regardless of M and v' is consistent with the similar T-shape structures of the three MCN. The ab initio calculation of LiNC also indicates that several superexcited ion-pair states have linear geometries. The potential-energy difference between the equilibrium structures of the ground and the superexcited ion-pair states is estimated to be 0.2 eV or larger, by considering the average rotational energy of the $CN(B^2\Sigma^+)$ product (0.2 eV).

V. CONCLUSIONS

The inverted vibrational and rotational excitation of $CN(B^2\Sigma^+)$ produced in the dissociative excitation of MCN in collision with Kr^m was explained by a large geometric change during the predissociation of MCN. The predissociative state is the superexcited ion-pair state diabatically correlating to $CN^-(3^1\Sigma^+)$ + M^+. The C−N internuclear distance of the

predissociative state is longer than that of the initial ground state of MCN so that the $CN(B^2\Sigma^+)$ product has the inverted vibrational distribution peaked at $v' = 1$. The rotational excitation is also driven by the in-plane geometric change during the dissociative excitation from the ground (T-shape) to the predissociative (linear) states. On the other hand, when RbCN and KCN are excited by Ar^m, which has larger excitation energies than Kr^m by ∼1.6 eV, the vibrational distribution of the $CN(B^2\Sigma^+)$ product is also inverted as populating in the range of $v' = 11-19$, the average vibrational energy of which is larger than that in the reaction with Kr^m by ∼3 eV. The rotational distribution of the $CN(B^2\Sigma^+)$ product in the reaction of Ar^m is statistical in contrast to the inverted rotational distribution in the present reaction. In spite of the small difference in the excitation energy between Kr^m and Ar^m as well as the high density of states of the superexcited states, the excitation is selective and characteristic of the predissociative superexcited ion-pair states involved, leading to the completely different energy partitions.

■ AUTHOR INFORMATION

Corresponding Author

Hisato Yasumatsu − *Cluster Research Laboratory, Toyota Technological Institute: in East Tokyo Laboratory, Genesis Research Institute, Inc., Chiba 272-0001, Japan;* orcid.org/0000-0001-9546-8869; Phone: +81-47-320-5915; Email: yasumatsu@clusterlab.jp

Author

Gwang-Hi Jeung − *Institut des Sciences Moléculaires de Marseille, Service 561, Campus de Saint-Jérôme, Aix-Marseille Université, Marseille 13397, France*

Notes

The authors declare no competing financial interest.

■ ACKNOWLEDGMENTS

We would like to sincerely express gratitude to the late Professor Tamotsu Kondow (Toyota Technological Institute) for his invaluable advice and support of the present research. One of the authors, H.Y., is grateful to Professor Suehiro Iwata (Keio University) for discussion on the ab initio calculations of CN^- and to Professor Haruhiko Ito (Nagaoka University of Technology) for providing us the RKR potential energy curve of $CN(B^2\Sigma^+)$. H.Y. also acknowledges Université de Provence (Aix-Marseille Université since 2012) for the invitation as Professeur Invité. This research was supported by the Special Cluster Research Project of Genesis Research Institute, Inc. and Grant-in-Aid for General Scientific Research from the Ministry of Education, Science and Culture.

■ REFERENCES

(1) Illenberger, E.; Momigny, J. *An Introduction to Elementary Processes Induced by Ionization*; Springer-Verlag: New York, 1992.

(2) Hatano, Y. In *Dynamics of excited molecules*; Kuchitsu, K., Ed.; Elsevier: Amsterdam, 1994, Chapter 6.

(3) Bowling, R. A.; Allen, J. D., Jr.; Schweitzer, G. K. The HeI photoelectron spectra of gaseous alkali cyanides. *J. Electron Spectrosc. Relat. Phenom.* **1979**, *16*, 489−491.

(4) Lee, D.-K.; Lim, I. S.; Lee, Y. S.; Hagebaum-Reignier, D.; Jeung, G.-H. Molecular properties and potential energy surfaces of the cyanides of the groups 1 and 11 metal atoms. *J. Chem. Phys.* **2007**, *126*, 244313.

(5) Lee, D.-K.; Lee, Y. S.; Hagebaum-Reignier, D.; Jeung, G.-H. First-order correction for bond energy applied to polar molecules: Alkali halides, alkali cyanides, $LiCH_3$, and CH_3F. *Chem. Phys.* **2006**, *327*, 406−414.

(6) Yasumatsu, H.; Jeung, G.-H. Ab initio study on electronically excited states of lithium isocyanide, LiNC. *Chem. Phys. Lett.* **2014**, *591*, 25−28.

(7) Yasumatsu, H.; Kondow, T.; Suzuki, K.; Tabayashi, T.; Shobatake, K. Absorption spectra of alkali cyanide molecules in the vacuum-ultraviolet region: transitions to dissociative and predissociative states. *J. Phys. Chem.* **1994**, *98*, 1407−1410.

(8) Yasumatsu, H.; Kondow, T.; Suzuki, K. Vibrational distributions of the $CN(B^2\Sigma^+)$ produced in the dissociative excitation of potassium cyanide and sodium cyanide with argon metastable atoms: bimodal vibrational distribution from potassium cyanide. *J. Phys. Chem.* **1993**, *97*, 6788−6792.

(9) Yasumatsu, H.; Suzuki, K.; Kondow, T. Production of vibrationally excited $CN(B^2\Sigma^+)$ via superexcited ion-pair state of triatomic alkali-metal cyanides by $Ar(^3P_{2,0})$ Impact. *J. Phys. Chem. A* **1998**, *102*, 7217−7221.

(10) Skudlarski, K.; Miller, M. Mass-spectrometric studies of sodium and potassium cyanides. *High Temp. Sci.* **1982**, *15*, 151−163.

(11) Kanda, K.; Ito, H.; Someda, K.; Suzuki, K.; Kondow, T.; Kuchitsu, K. Violet emission of cyanogen produced in the reaction of argon$(^3P_{2,0})$ with cyanogen bromide. 1. Nascent vibrational and rotational distributions of $CN(B^2\Sigma^+)$. *J. Phys. Chem.* **1989**, *93*, 6020−6024.

(12) Sobczynski, R.; Setser, D. W. Improvements in the generation and detection of $Kr(^3P_0)$ and $Kr(^3P_2)$ atoms in a flow reactor: Decay constants in He buffer and total quenching rate constants for Xe, N_2, CO, H_2, CF_4, and CH_4. *J. Chem. Phys.* **1991**, *95*, 3310−3324.

(13) L'vov, B. V.; Pelieva, L. A. Thermodynamics study of gaseous monocyanides by electrothermal atomic absorption spectrometry. *Prog. Anal. Atom. Spectrosc.* **1980**, *3*, 65−86.

(14) DeLong, M. C.; Rosenberger, F. High purity cyanides: A dying technology revived. *J. Cryst. Growth* **1986**, *75*, 164−172.

(15) Bauer, E.; Fisher, E. R.; Gilmore, F. R. De-excitation of Electronically Excited Sodium by Nitrogen. *J. Chem. Phys.* **1969**, *51*, 4173−4181.

(16) Zhu, C.; Nakamura, H. The two-state linear curve crossing problems revisited. III. Analytical approximations for Stokes constant and scattering matrix: Nonadiabatic tunneling case. *J. Chem. Phys.* **1993**, *98*, 6208−6222.

(17) Olson, R. E.; Smith, F. T.; Bauer, E. Estimation of the Coupling Matrix Elements for One-Electron Transfer Systems. *Appl. Opt.* **1971**, *10*, 1848−1855.

(18) Huber, H.; Herzberg, G. *Molecular Spectra and Molecular Structure IV. Constants of Diatomic Molecules*; Van Nostrand Reinholt: New Jersey, 1979.

(19) Lu, R.; Halpern, J. B.; Jackson, W. M. Photodissociation of C_2N_2, chlorine cyanide (ClCN), and bromine cyanide (BrCN) in a pulsed molecular beam. *J. Phys. Chem.* **1984**, *88*, 3419−3425.

(20) van Vaals, J. J.; Meerts, W. L.; Dymanus, A. High-resolution molecular-beam spectroscopy of NaCN and $Na^{13}CN$. *Chem. Phys.* **1984**, *86*, 147−159.

(21) van Vaals, J. J.; Meerts, W. L.; Dymanus, A. Molecular beam electric resonance study of KCN, $K^{13}CN$ and $KC^{15}N$. *J. Mol. Spectrosc.* **1984**, *106*, 280−298.

(22) Marsden, C. J. Abinitio correlated potential energy surfaces for monomeric sodium and potassium cyanides. *J. Chem. Phys.* **1982**, *76*, 6451−6452.

(23) van Leuken, E.; Brocks, G.; Wormer, P. E. S. An SCF potential energy and dipole surface for rubidium cyanide (RbCN). *Chem. Phys.* **1986**, *110*, 365−373.